Li, Guoxing, Gu, Fengshou, Wang, Tie, Zhang, Ruiliang and Ball, Andrew

A Dynamic Deformation based Lubrication Model between the Piston Rings and Cylinder Liner

Proceedings of the 23rd International Conference on Automation & Computing, University of Huddersfield, Huddersfield, UK, 7-8 September 2017

A Dynamic Deformation based Lubrication Model between the Piston Rings and Cylinder Liner

Guoxing Li[1], Fengshou Gu[2], Tie Wang[3]*, Xingchen Lu[4], Ruiliang Zhang[5], Andrew Ball[6]
[1, 2, 3 ,4, 5] Department of Vehicle Engineering, Taiyuan University of Technology, Taiyuan, P.R. China
[1, 2, 6] Centre for Efficiency and Performance Engineering, University of Huddersfield, UK
[3*]Corresponding author： *wangtie57@163.com*

***Abstract*— The piston ring-cylinder liner friction pair is one of the most important friction pair in IC engines. In previous modelling studies, most researches were carried out based on a hypothesis that the inner surface of liner is an ideal cylindrical shell without considering the effects of dynamic deformation on oil film distribution. To investigate the potential influences of structural deformations on tribological behaviors of cylinder assemblies, the dynamic deformation of liner surface was obtained by FEM-based dynamic simulation, and then introduced into the lubrication model. Different from the traditional lubrication model where the pressure stress factor and shear stress factor are regarded as constant, this paper calculated these factors in real time by numerical integration to achieve more realistic simulation results. This study shows that the friction force obtained from the improved model manifests obvious fluctuations, and shows a significant reduction compared to original model.**

Keywords- dynamic deformation; cylinder liner; piston ring; oil film lubrication; friction force

I. Introduction

The tribological behaviour of piston and rings assembly has long been recognized as an important influence factor on the performance of internal combustion (IC) engines in terms of fuel consumption, power loss, harmful exhaust emissions and blow-by [1]. Figure 1 shows a typical distribution of the total engine mechanical friction losses for a diesel engine. It can be seen that the piston and ring assembly accounts for the largest proportion 45~50% of friction losses in a diesel engine [2]. To improve the fuel efficiency and extend the engine service life, it is essential to detailed model the friction and lubrication behaviours between the piston rings and cylinder liners of IC engines.

Research on modelling of piston ring-cylinder liner tribological behaviours has been developed for decades. In modelling oil film formation and distribution on the cylinder liners, the cylinder wall is often taken as being a perfect cylindrical surface by the majority of researchers [3]–[6]. However, no cylinder liner is perfectly cylindrical or of nominal bore radius along its entire length. The liner distortion leads to loss of conformity between the piston rings and cylinder liner. As a result of liner deformation, the drop of piston ring follow-up performance can cause the uneven contact and varied friction [7].

The project of this paper is supported by Natural and Scientific foundation of China.(NO. 51375326).

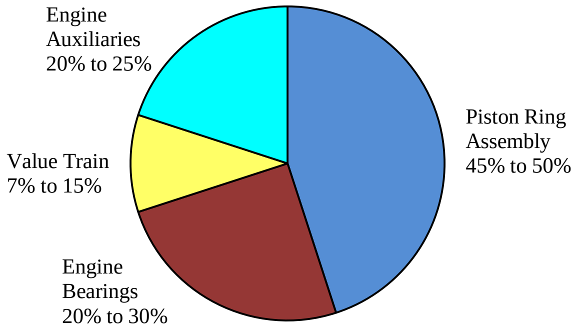

Figure 1. Distribution of the total mechanical losses of a diesel engine [2]

A study conducted by Usman et al. [8] pointed out that a distorted cylinder liner will decrease the viscous friction force between the piston ring and cylinder liner surfaces because the average film thickness between a distorted liner and ring is much higher than that between a circular liner and ring. Ning et al. [9] conducted a numerical study involving the piston and liner system lubrication considering the thermal and elastic deformation of the cylinder liner, showing that with considering the effects of liner thermal distortions, the piston and liner assembly may run in a safer situation because the minimum oil film thickness (MOFT) is thicker than the original model by up to 20%, and the friction losses are correspondingly decreased by approximately 4% than the original prediction.

However, all of these attempts to introduce liner deformations into lubrication model are confined to the category of static deformation or quasi-static deformation. There is no high-frequency modal -related deformation has been introduced into the lubrication model yet. According to the simulation results obtained by G. Li and F. Gu [10], the amplitude of liner deformations induced by piston slaps is at the order of 0.1 microns, being about 20% of the roughness amplitude, which may affect the distribution of oil film. To examine the influences of dynamic deformation on lubrication performance and the friction loss of liners, this paper improves the existing lubrication model by introducing dynamic deformations of liner surface.

II. Simulation of Surface Dynamic Deformation

A. Establishment of Finite Element Model

Figure 2 shows the three-dimensional model of a single-cylinder engine. To facilitate the viewing of simulation results, the cylinder block is set to be transparent. The cylinder liner studied in this paper is made of ductile cast iron QT600-3. The material parameters are listed in Table I.

To obtain the instantaneous deformations on the flanges at top end and the overall cylindrical shell, the model was configured to have 7121 hexahedral isoparametric solid elements using ANSYS Workbench. To reduce the need for solution time and computing sources, all the other components are treated as rigid body in modelling.

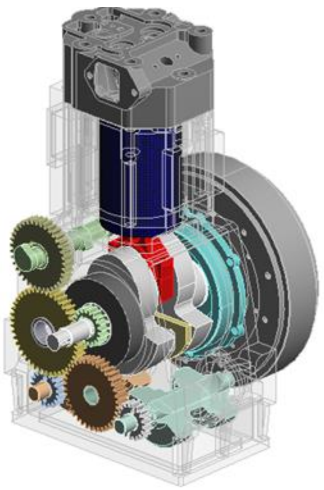

Figure 2. Finite element model of cylinder assembly

TABLE I. Material properties of QT600-3

Density (kg/m³)	*Young's Modulus(Pa)*	*Poisson's Ratio*	*Bulk Modulus (Pa)*	*Shear Modulus (Pa)*
7120	1.69e+11	0.286	1.316e+11	6.5708e+10

Excitation configurations:

(1) The combustion pressure data collected by the in-cylinder pressure sensor were introduced into the finite element model as the combustion excitation.

(2) In order to simulate the dynamic deformation of the cylinder liner excited by piston knocks, the piston side-thrust force was calculated according to [10], and the calculated force was applied to the piston to strike the cylinder liner laterally.

B. Numerical Evaluations

For a better understanding of liner dynamic responses to two excitations, a numerical analysis was carried out based on the established model under an input of either the combustion force or piston slap force. Figure 3 presents two typical responses respective to the combustion shock and piston slap, at crank angle of 370°.

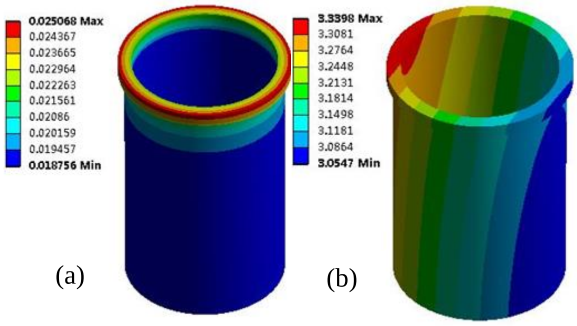

Figure 3. Total deformation of cylinder liner (Unit: mm)

It can be seen in Figure 3(a) that the significant deformation response to combustion shock is mainly appeared and concentrated in the top portion of the liner, while the response to piston slap extended throughout the entire liner structure, as seen in Figure3 (b). As these deformations include the quasi-static deformation due to the effect of elastic constraints, the absolute magnitudes of maximum deformation reach to about 25 microns and 0.5 millimetre. After removing translation movement and the quasi-static deformations, especially that of Figure3 (b), the magnitude information of high-frequency local deformations can be obtained. The predicted amplitude of local responses is in the order of 0.02 microns due to the combustion shock, which may be negligible in predicting lubrications between the piston ring and the liner as it far less than the roughness magnitudes of the lubricated surfaces. However, piston slaps can lead to deformation as high as 0.1 micron, being about 20% of roughness amplitude.

III. Development of Dynamic Deformation Based Lubrication Models

As mentioned above, the amplitude of liner deformations induced by piston slaps is at the order of 0.1 microns, being about 20% of the roughness amplitude, this may change the distribution of oil film and thus affect the lubrication behaviour. Therefore, it is essential to take the dynamic deformation into account in the existing oil film models.

A. Governing Eqution

1) Average Reynolds Equation

In a mixed lubrication regime, Patir and Cheng's average Reynolds equation [11] describes the isothermal, incompressible lubricant behaviour between the ring and liner rough surfaces

$$\frac{\partial}{\partial x}\left(\emptyset_x \frac{h^3}{\eta}\frac{\partial \bar{p}}{\partial x}\right)+\frac{\partial}{\partial y}\left(\emptyset_y \frac{h^3}{\eta}\frac{\partial \bar{p}}{\partial y}\right)$$
$$=6U\frac{\partial(\bar{h}_T)}{\partial x}+6U\sigma\frac{\partial(\emptyset_s)}{\partial x}+12\frac{\partial(\bar{h}_T)}{\partial t} \quad (1)$$

where ϕ_x, ϕ_y are pressure flow factors, ϕ_s is the shear flow factor, $\bar{p}$ is the mean pressure, and σ is the composite RMS roughness of ring and liner, U is the piston primary velocity, η is the lubricant viscosity.

2) Asperity Contact

Surface asperities contact occurs only when the hydrodynamic pressure is insufficient to separate two matching surfaces. Greenwood-Tripp's rough surface contact model estimated the asperity contact load based on the surface mean separation and other statistical parameters [6]. The average contact pressure P_a was related to the density of asperities μ, the curvature of asperity of radius β, composite surface roughness σ, and composite material modulus E.

$$P_a(h) = \frac{16\sqrt{2}}{15}\pi(\sigma\beta\mu)^2 E\sqrt{\frac{\sigma}{\beta}}F_{2.5}\left(\frac{h}{\sigma}\right) \quad (2)$$

where:

$$F_{2.5}(x) = \frac{1}{\sqrt{2\pi}}\int_x^{\infty}(s-x)^{2.5}e^{-s^2/2}\,ds \quad (3)$$

$$\frac{1}{E} = \frac{1-v_1^2}{E_1} + \frac{1-v_2^2}{E_2} \quad (4)$$

In equations (2) to (4), E_1 and E_2 are ring and liner Young's modulus, and v_1 and v_2 are ring and liner Poisson's ratio.

3) Calculation of The Frictional Force

The shearing of asperities and viscous lubricant film generates the friction force in the mixed lubrication regime. Viscous friction is attributed to generated shear stress arising from entraining motion of the lubricant as well as pressure gradient in a converging–diverging wedge. The hydrodynamic component of average friction force F_h can be predicted by an integration of viscous shear stress across the sliding surfaces.

$$F_h = \int_A \tau dA \quad (5)$$

Furthermore, to meet different sliding scenarios, the local shear stress τ can also be expressed in terms of the mean quantities and three empirical shear stress factors ϕ_f, ϕ_{fp} and ϕ_{fs}.

The asperity component of friction force is caused by contact between the ring surface and cylinder wall.

$$F_a = \mu_f \int_{-B/2}^{B/2} P_a\,dx \quad (6)$$

where μ_f is the friction coefficient under lubricated contact (boundary lubrication). B is the ring axial thickness.

The total friction force between the piston ring and the cylinder liner is synthesized by two components

$$F_f = F_h + F_a \quad (7)$$

The key parameters used in this study are given in Table II, in which the surface parameters are obtained from the engine manufacturer.

TABLE II. VALUES OF PARAMETERS FOR SIMULATION

Symbol	***Nomenclature***	***Value***
σ_1	Cylinder surface roughness	0.8 µm
σ_2	Ring surface roughness	0.4 µm
r	Crank radius	0.057 m
l	Connecting rod length	0.19 m
e_1	Piston ring surface height	0.003 m
B	The axial height of piston ring	0.003 m
ρ	Oil density	890 Kg/m^3
E_1	Liner elastic modulus	122×10^9 Pa
E_2	Modulus of elasticity of piston rings	165×10^9 Pa

B. *Improved Film Thickness with Consideration of Cylinder Deformation*

For the mathematical model, the initial film thickness and film profile are predefined. During the computation, the contour of film distribution is changeless; only the thickness of the overall film surface is modified to adjust the bearing capacity of the film or asperities for achieving overall force balance.

Therefore, introducing the dynamic deformations of liner surface, in the form of a predefined condition, into the calculation, will not change the core algorithm of Reynolds equations, and will not produce any adverse effect on the accuracy of the model.

Figure 4 depicts a conjunction between the piston ring and cylinder liner with surface roughness. Here the function $h_T(x)$ describes the local film thickness, including surface roughness.

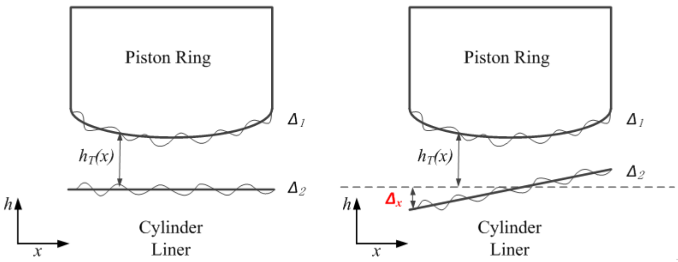

Figure 4. Rough piston ring and cylinder liner conjunction: (1) without liner deformation (2) with consideration of liner deformation

For one-dimensional lubrication, the local film thickness h_T is given by

$$h_T = h + \Delta_1 + \Delta_2 \quad (8)$$

Where h is the nominal film thickness, Δ_1 is the surface roughness amplitude of piston ring, Δ_2 is the surface roughness amplitude of cylinder liner. The nominal thickness$h = h_{min}(t) + h_x(x)$, giving

$$h_T(t) = h_{min}(t) + h_x(x) + \Delta_1 + \Delta_2 \quad (9)$$

Taking the deformation amplitude of the liner surface Δ_x into account in the film formation model, the nominal film thickness can be improved as

$$h_{T_{deforms}}(t) = h_{min}(t) + h_x(x) + \Delta_1 + \Delta_2 + \Delta_x = h_T(t) + \Delta_x \quad (10)$$

By analogy, for the two-dimensional lubrication, the film thickness is given by

$$h_{T_{deforms}}(t) = h_{min}(t) + h_x(x) + h_y(y) + \Delta_1 + \Delta_2 + \Delta_x + \Delta_y = h_T(t) + \Delta_x(t) + \Delta_y(t)$$

$$= h_T(t) + \Delta_{deforms}(t) \tag{11}$$

where, the two-dimensional deformation of the liner surface matched with the piston ring is combined with axial deformation Δ_x and circumferential deformation Δ_y.

C. *Improved Stress Factors with Consideration of Cylinder Deformation*

Patir and Cheng [12] developed stress factors that modify the predicted shear stress acting on a rough surface in a highly viscous flow. The average shear stress is given by

$$\tau = \frac{\mu U}{h}(\phi_f - \phi_{fs}) + \phi_{fp}\frac{h}{2}\left(\frac{\partial p}{\partial x}\right) \tag{12}$$

where τ is the shear stress acting on the ring surface, ϕ_f is a geometric factor, ϕ_{fs} and ϕ_{fp} are the shear stress and press stress factor, respectively.

All stress factors proposed by Patir and Cheng are only applicable to artificial Gaussion random rough surfaces, and these factors are constants over the entire surface. However, the cylinder liner surface are highly non-Gaussion when considering the dynamic deformation close to the order of surface roughness, and the shear stress τ is not equal everywhere. Therefore, the local stress factors should be calculated locally and real-timely.

It is necessary to mesh the solve region of ring surface with $m \times n$ nodes, and to solve the local stress factors in the discrete domain using the finite difference method. The m and n are the respective number of nodes in the axial and circumferential directions. Figure5 shows surface interpolation between nodes for stress factor calculation.

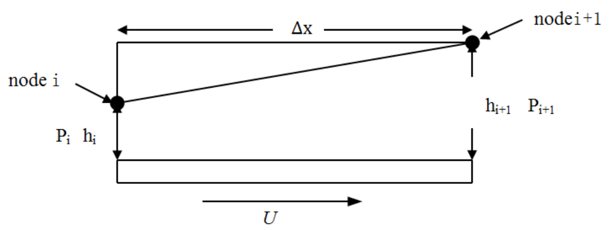

Figure 5. Surface interpolation between nodes for stress factor calculation[13]

The geometric stress factor are functions only of rough surface geometry, is defined by

$$\phi_f = h \cdot \frac{1}{m(n-1)} \sum_{i=1}^{n-1} \sum_{j=1}^{m} \frac{\ln(h_i/h_{i+1})}{h_i - h_{i+1}} \tag{13}$$

ϕ_{fp} is a correction factor for the mean pressure stress component of the shear stress, is defined by

$$\phi_{fp} = \frac{\frac{1}{m(n-1)} \sum_{i=1}^{n-1} \sum_{j=1}^{m} \frac{2h_i h_{i+1}(P_{i+1,j} - P_{i,j})}{(h_i + h_{i+1})\Delta x}}{\frac{h}{2}\frac{dP}{dx}} \tag{14}$$

ϕ_{fs} is another correction term which arises from the combined effect of roughness and sliding, is defined by

$$\phi_{fs} = \frac{\frac{1}{m(n-1)} \sum_{i=1}^{n-1} \sum_{j=1}^{m} \frac{h_i h_{i+1}(P_{i+1,j} - P_{i,j})}{(h_i + h_{i+1})\Delta x}}{\frac{\mu U}{h}} \tag{15}$$

Substituting (13), (14), (15) into (12), then τ can be expressed as

$$\tau = \frac{1}{m(n-1)} \sum_{i=1}^{n-1} \sum_{j=1}^{m} \begin{bmatrix} \mu U \cdot \frac{\ln(h_i/h_{i+1})}{h_i - h_{i+1}} + \\ \frac{1}{2}\frac{(P_{i+1,j} - P_{i,j})}{\Delta x} \cdot \frac{2h_i h_{i+1}}{h_i + h_{i+1}} \end{bmatrix} \tag{16}$$

Where $H_{fp} = \frac{2h_i h_{i+1}}{h_i + h_{i+1}}$, $H_{fs} = \frac{h_i - h_{i+1}}{\ln(h_i/h_{i+1})}$ are the equivalent heights used to calculate the corresponding local shear stress due pressure and shear stress, respectively.

Then, the average shear stress is given by

$$\tau = \frac{1}{m(n-1)} \sum_{i=1}^{n-1} \sum_{j=1}^{m} \left[\frac{\mu U}{H_{fs}} + \frac{H_{fp}}{2}\frac{(P_{i+1,j} - P_{i,j})}{\Delta x}\right] \tag{17}$$

Substituting the improved average shear stress equation into equation (5), the viscosity friction force between piston ring and liner can be calculated in real time.

IV. RESULTS AND DISCUSSION

After running throughout an entire working cycle, the minimum oil film thickness H_{min} and friction forces versus the crank angle with and without consideration of dynamic deformations can be obtained as seen in Figure 6 and Figure 7.

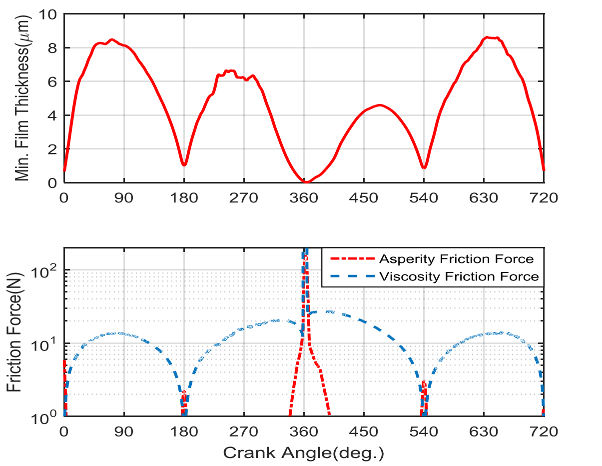

Figure 6. Minimum oil film thickness and friction force of compression ring

Figure6 shows the minimum oil film thickness H_{min} for the top compression ring versus the crank angle. The lowest minimum oil film thickness occurs in the vicinity of the dead centres which correspond to crank angles of 0, 180, 360, and 540 degrees. This prediction agrees with the wear pattern observed on the cylinder-liner interface, which shows serious wear at the top and bottom of the piston stroke. The peak of minimum oil film thickness occurs at the middle of the piston stroke, where the maximum hydrodynamic action is attained.

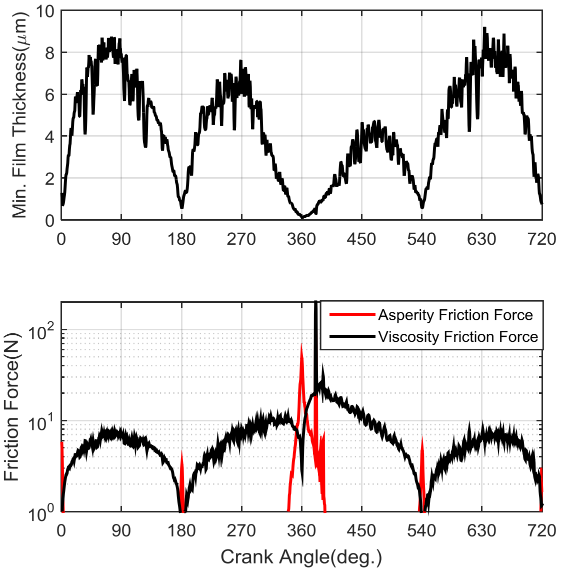

Figure 7. Minimum oil film thickness and friction force considering dynamic deformation

As shown in Figure 7, the minimum oil film thickness H_{min} considering the dynamic deformation of the cylinder liner shows significant fluctuations throughout the entire operating cycle, especially in the mid-strokes with higher sliding speed. The friction curves of the improved model also manifest some obvious fluctuations. This indicates that the friction and lubrication process of the piston ring-liner pair can indeed be affected by the dynamic deformations of cylinder liners.

For comparing and analysing the influence of liner deformations to lubrication behaviours, the predicted minimum oil film thickness and friction forces with and without consideration of dynamic deformations, are drawn together in Figure 8.

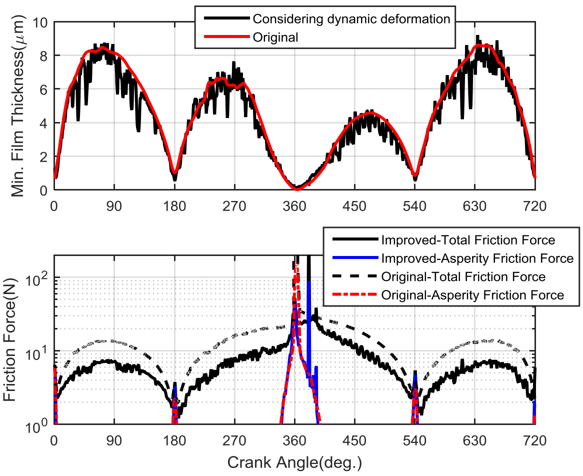

Figure 8. Comparison of friction force between the improved and original

The improved minimum oil film thickness H_{min} after combustion TDC (Top Dead Centre) is slightly fluctuated around the original one, while its corresponding friction force presents some more complex and significant changes in the power stroke, as shown in Figure 8. This may indicate that the actual friction and wear behaviours between piston rings and liners are far more complex than had been previously theoretically estimated.

In the middle of the piston stroke, the improved friction force, mainly the viscous friction force, shows an obviously decline compared to the original one. This kind of friction reduction may be attributed to the increase of shear stress factor ϕ_{fs}, as a result of the introduction of surface dynamic deformations. ϕ_{fs} is the correction factor for the combined effect of sliding roughness on the shear force[12]. With the increase of ϕ_{fs}, the difference between the sliding velocity correction factor ϕ_f and shear stress factor ϕ_{fs} subsequently exhibited obvious decrease, as seen in equation 12. Therefore, the local shear stress τ can be reduced accordingly, with the introducing of liner dynamic deformations.

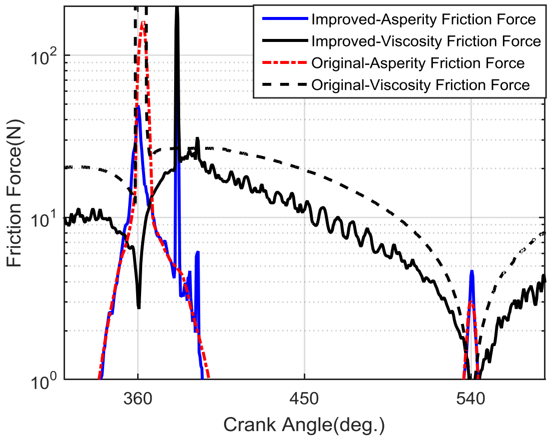

Figure 9. Partial magnification

As seen in Figure 9, around the combustion TDC at 360°, the value of asperity friction considering liner deformation is lower than that of original model. Due to the introduction of dynamic deformation, the lubricating condition between the matched surfaces is improved, with the help of emergence of many local surface pits and its resulting reduction of the effective contact area of the asperity contact. This might indicate that the dynamic deformation of the liner can help to reduce the asperity friction near the combustion TDC, normally regarded as the most serious position of wear, and to enhance the operation efficiency and service life of engines.

V. CONCLUSIONS

In the paper, an improved lubrication model of the top compression ring and cylinder liner considering the influence of liner dynamic deformation on lubrication behaviours has been presented. The related conclusions can be made as follows:

- The minimum oil film thickness and friction forces predicted by the improved model manifest obvious fluctuations, indicates that the lubrication behaviours between the piston rings and liners can indeed be affected by the dynamic deformations of cylinder structures.

- The friction forces predicted by improved model show a significant reduction with respect to that of original model. This suggests that the dynamic deformations of the liner surface might be beneficial to reduce the friction losses and to enhance the operational efficiency of IC engines.

- The asperity friction force obtained from improved model shows an obvious decline around the combustion TDC compared to the original model, as a result of the reduced effective contact area of the asperity contact.

REFERENCES

[1] M. Kapsiz, M. Durat, and F. Ficici, “Friction and wear studies between cylinder liner and piston ring pair using Taguchi design method,” *Adv. Eng. Softw.*, vol. 42, no. 8, pp. 595–603, Aug. 2011.

[2] A. Comfort, “An Introduction to Heavy-Duty Diesel Engine Frictional Losses and Lubricant Properties Affecting Fuel Economy - Part 1,” Dec. 2004.

[3] B. C. Majumdar and B. J. Hamrock, “Effect of surface roughness on hydrodynamic bearings,” *NASA TM-81711 Oct*, vol. 9, 1981.

[4] Y. Hu, H. S. Cheng, T. Arai, Y. Kobayashi, and S. Aoyama, “Numerical Simulation of Piston Ring in Mixed Lubrication—A Nonaxisymmetrical Analysis,” *J. Tribol.*, vol. 116, no. 3, pp. 470–478, Jul. 1994.

[5] O. Akalin and G. M. Newaz, “Piston Ring-Cylinder Bore Friction Modeling in Mixed Lubrication Regime: Part I—Analytical Results,” *J. Tribol.*, vol. 123, no. 1, pp. 211–218, 1999.

[6] J. A. Greenwood and J. H. Tripp, “The Contact of Two Nominally Flat Rough Surfaces,” *Proc. Inst. Mech. Eng.*, vol. 185, no. 1, pp. 625–633, Jun. 1970.

[7] P. Andersson, J. Tamminen, and C.-E. Sandström, “Piston ring tribology,” *Lit. Surv. VTT Tied.-Res. Notes*, vol. 2178, no. 1, 2002.

[8] A. Usman, T. A. Cheema, and C. W. Park, “Tribological performance evaluation and sensitivity analysis of piston ring lubricating film with deformed cylinder liner,” *Proc. Inst. Mech. Eng. Part J J. Eng. Tribol.*, vol. 229, no. 12, pp. 1455–1468, Dec. 2015.

[9] L. Ning, X. Meng, and Y. Xie, “Incorporation of deformation in a lubrication analysis for automotive piston skirt–liner system,” *Proc. Inst. Mech. Eng. Part J J. Eng. Tribol.*, vol. 227, no. 6, pp. 654–670, Jun. 2013.

[10] G. Li, F. Gu, N. Wei, Y. Xu, A. D. Ball, and T. Wang, “A validated finite element model for predicting dynamic responses of cylinder liners in an IC engine,” 2016, pp. 126–131.

[11] N. Patir and H. S. Cheng, “An Average Flow Model for Determining Effects of Three-Dimensional Roughness on Partial Hydrodynamic Lubrication,” *J. Tribol.*, vol. 100, no. 1, pp. 12–17, Jan. 1978.

[12] N. Patir and H. S. Cheng, “Application of Average Flow Model to Lubrication Between Rough Sliding Surfaces,” *J. Tribol.*, vol. 101, no. 2, pp. 220–229, Apr. 1979.

[13] J. J. A. Jocsak, “The effect of surface finish on piston ring-pack performance in advanced reciprocating engine systems,” Massachusetts Institute of Technology, 2005.